Hydrodynamic Model of Temperature Change in Open Ionic Channels

Duan P. Chen,* Robert S. Eisenberg,* Joseph W. Jerome,‡ and Chi-Wang Shu§

*Department of Molecular Biophysics and Physiology, Rush Medical College, Chicago, Illinois 60612; ‡Department of Mathematics, Northwestern University, Evanston, Illinois 60208; and §Division of Applied Mathematics, Brown University, Providence, Rhode Island 02912 USA

ABSTRACT Most theories of open ionic channels ignore heat generated by current flow, but that heat is known to be significant when analogous currents flow in semiconductors, so a generalization of the Poisson–Nernst–Planck theory of channels, called the hydrodynamic model, is needed. The hydrodynamic theory is a combination of the Poisson and Euler field equations of electrostatics and fluid dynamics, conservation laws that describe diffusive and convective flow of mass, heat, and charge (i.e., current), and their coupling. That is to say, it is a kinetic theory of solute and solvent flow, allowing heat and current flow as well, taking into account density changes, temperature changes, and electrical potential gradients. We integrate the equations with an essentially nonoscillatory shock-capturing numerical scheme previously shown to be stable and accurate. Our calculations show that 1) a significant amount of electrical energy is exchanged with the permeating ions; 2) the local temperature of the ions rises some tens of degrees, and this temperature rise significantly alters the ionic flux in a channel 25 Å long, such as gramicidin-A; and 3) a critical parameter, called the saturation velocity, determines whether ionic motion is overdamped (Poisson–Nernst–Planck theory), is in an intermediate regime (called the adiabatic approximation in semiconductor theory), or is altogether unrestricted (requiring the full hydrodynamic model). It seems that significant temperature changes are likely to accompany current flow in the open ionic channel.

INTRODUCTION

Ion channels are porous proteins inserted across cell membranes that translocate ions selectively from one side of the membrane to the other. The pores of channel proteins are tens of angstroms long and a few angstroms in radius and so are small enough to be selective among different ion species (Hille, 1992). Ionic movement has long been modeled in two traditions, that of diffusion theory and that of activated barrier crossing, i.e., rate theory. Diffusion theory in particular, and both theories in general, usually assume isothermal systems, systems with constant temperature everywhere. Flux in a condensed phase invariably produces heat, of course, but the heat generated has been assumed to be small and of little consequence.

The movement of current (specifically, holes and electrons) in semiconductors has been modeled by diffusion theory for nearly 50 years, again assuming constant temperature in most cases. For at least 30 years it has been clear that local temperature changes occur and produce important phenomena in semiconductor devices (Stratten, 1962), and a theory has been developed to describe, explain, and predict such "hot electron" phenomena. Here we apply that theory to ionic channels: in particular, we compute the expected profiles of temperature in a channel, using the hydrodynamic theory of semiconductor physics, with parameters appropriate for ionic channels, to the extent that they are known. The lack of knowledge of parameters and constitutive laws for ions, waters, and atoms of the channel protein is the greatest source of uncertainty in this work.

Our calculations show substantial temperature changes under a wide range of conditions. Recent simulations of molecular dynamics (see the next section) and analysis of stochastic dynamics have shown rich behavior of ionic trajectories under physiological conditions, behavior not characteristic of friction-dominated (i.e., overdamped) or equilibrium systems. Our results suggest that temperature changes will be found in theory, simulation, and experiments once they are sought, and we hope that our results will motivate that work.

Rate theory is often used to describe flux over predetermined or separately determined potential barriers. We prefer the more general theory in which the permeation of ions across channels is described as a combination of drift and diffusion obeying the Poisson and Nernst–Planck equations simultaneously, called the PNP theory. It was introduced rigorously into the analysis of channels by Barcilon et al. (1992) and analyzed further by Chen and Eisenberg (1993a).

PNP theory assumes that ionic motion is overdamped. Specifically, it assumes that 1) the motion of ions is damped instantaneously by frequent collisions of ions with their surroundings and 2) the energy transfer in this damping is small, and consequently the collisions will not significantly change the temperature. In this theory, the functions of channel proteins are determined by the charge distributions on channel proteins (as well as by the mobile charge in the channel's pores) and their geometry. Thus, critical mutations of channel proteins can produce significant changes in channel function by changing the charge distribution along the protein. (Of course, they may change its shape, i.e., the conformation of the protein, as well.) However, this theory

Received for publication 21 October 1994 and in final form 9 May 1995.

Address reprint requests to Dr. Duan P. Chen, Department of Molecular Biophysics and Physiology, Rush Medical College, 1750 West Harrison Street, JS1298, Chicago, IL 60612-3824. Tel.: 312-942-5312; Fax: 312-942-8711; E-mail: duan@aix550.phys.rpslmc.edu.

0006-3495/95/12/2304/19 $2.00

by itself cannot deal with biological transport when energy is directly involved, for example, active transport.

We raise the question whether ion motion inside the channel is really overdamped. Gramicidin-A (Mackay et al., 1984; Fornili et al., 1984; Chiu et al., 1989; Roux and Karplus, 1991; Elber et al., 1994; Rosenberg and Finkelstein, 1978; Finkelstein and Andersen, 1981; Finkelstein, 1987; Levitt et al., 1978; Dani and Levitt, 1981; Levitt, 1984; Wallace, 1990; Smart et al., 1993) can accommodate eight to twelve water molecules at the same time. In other words, an ion, once it is inside a channel protein, is surrounded by far fewer water molecules than in bulk solution, and collisions with water molecules must occur much less frequently. Furthermore, an ion exchanges water for protein in its solvation shell as it enters a channel. Hydration and the concomitant free energy are lost, balanced—more or less well—by the ion's solvation energy once in the channel's pore. The change in energy is a kind of change in state, described (in the tradition of equilibrium electrochemistry) by different free energies of the standard state of equilibrium. That change in energy undoubtedly will be at the expense of the electrical energy supplied by the electric field and the kinetic energy of the ion itself. The change in kinetic energy will effectively change the temperature of ions.

Based on the above arguments, it is probably unwise to assume uniform temperature in ionic channels. Here we investigate the role of energy exchange within the channel in ion permeation by studying the natural extension of PNP theory, which is called the hydrodynamic model in the literature of the Boltzmann transport equation (Cercignani, 1988). The model contains an equation that describes the exchange of energy among ion, water, and channel protein, among the electric, temperature, and pressure fields. This energy equation includes heat flux, frictional loss, and work done both by ions themselves and by the external applied electric field.

As a beginning, we have studied a channel selective to one kind of ion species, say, a cation. Our results demonstrate that the nature of permeation is altered when ions are surrounded not by a shell but by a stream of water molecules. Significant exchange of energy is found between ions and the channel protein and between ions and the applied electric field. In particular, a significant temperature rise is found in the channel's pore. The properties of the channel protein, however, are independent of temperature in the present version of our model. Clearly temperature changes most properties of proteins, usually dramatically. Known temperature effects can easily be incorporated into our formulation. Unknown, they are better left out.

A critical physical quantity describing the frequency of collision divides the permeation of ions into three regimes: drift diffusion, in which no appreciable energy exchange occurs; a hydrodynamic regime, in which significant energy exchange occurs; and the intermediate situation of the adiabatic approximation.

We hope that our theory will motivate simulations and experiments: simulations of the molecular dynamics of channels seeking the basis for the parameters of the model used here, experiments measuring the predicted changes in temperature. We speculate that fluxes of different ions are likely to covary and to be coupled in that sense. In models like this, heat generated by hydrolysis of ATP (just outside a channel) can move ions against their concentration and electrical gradients and so can be the driving force for active transport.

HYDRODYNAMIC MODEL

The models discussed in this section can be viewed as macroscopic or microscopic, in the tradition of fluid dynamics or the kinetic theory of gases. It is instructive to present a brief survey here of the more classical work that starts from the Boltzmann transport equation of gases (see Eq. A.23 in the Appendix, reviewed in, for example, Chapman and Cowling, 1970), because it is significantly less difficult and so more convincing to the newcomer.

In the kinetic theory of gases (Huang, 1987) the hydrodynamic regime is defined when the mean free path is small compared with other length scales (as it surely is in solutions and channels). In this case the first three moments of the Boltzmann transport equation describe conservation of particle number, momentum, and energy, and the averaged (binary) collisions can be expressed by the relaxation time approximation, which appears as a friction (damping) term. It is not necessary to possess detailed information about the collisions when this approach is adopted. The entries of the pressure tensor (matrix) are computed by multiplying the components of random velocity, integrating them, and forming the product with the mass density; the heat conduction term is computed by multiplying the energy of random motion by random velocity, integrating, and forming the mass density product. The precise definitions are given in the Appendix. By assuming that the pressure tensor is isotropic—i.e., that the product of distinct random velocity components is, on the average, zero and its trace is equidistributed—we obtain two advantages: 1) Random kinetic energy and thermal energy are related as they are for independent particles, i.e., as in the ideal gas law, because the effective temperature is defined as proportional to the average random kinetic energy; 2) Viscosity, as defined by a second derivative of the velocity in fluid mechanics, does not enter explicitly into the momentum equation. Of course, frictional phenomena, characteristic of "thick" fluids such as honey, are present because of the relaxation terms of the model.

A moment method also yields a continuum model, extending well beyond the domain of dilute gases (Resibois and Leener, 1977). The resulting modification in the continuum, or hydrodynamic model, from that derived from the Boltzmann equation is reflected in the relaxation approximation. Specifically, this moment procedure produces a

model formally identical to the hydrodynamic model; the ultimate distinctions reside only in details of the particular relaxation approximation to the collision terms. Thus, more-recent work seeks a more-general starting point than the classical Boltzmann transport equation. It seeks a starting point less intimately connected with the idea of a binary collision (e.g., Bird, 1994; Smith and Jensen, 1989; McCourt et al., 1990; Beris and Edwards, 1994; Spohn, 1991; Mason and McDaniel, 1988).

In the hydrodynamic theory, the usual (Fourier) law of heat is derived from moments of the Boltzmann transport equation (see Huang, 1987). The heat conductivity is proportional to the particle concentration and mobility (see Blatt, 1968, where the expression is termed the Wiedemann–Franz law). The coefficient κ in the Wiedemann–Franz law is a direct consequence of the equipartition theorem for independent particles, which states that the average kinetic energy of such particles is $(3/2)k_BT$, where k_BT is the thermal energy. Notice that this term appears in the Appendix. The use of the Fourier law alone to describe the heat flux is discussed fully by Stettler et al. (1993).

It seems easy and obvious—well within our traditional thoughts—to describe solutions, or ions as independent particles, as they are described in classical channology and in the hydrodynamic theory. Unfortunately, when we turn to relaxation times little tradition is available to help us: experimental measurements, simulations, or theories of relaxation processes in channel proteins are not available, and little is known about proteins, or about ionic solutions for that matter. For that reason we use the temperature-dependent expressions in the simulation of semiconductor devices, knowing full well that they need new experimental, numerical, or theoretical justification when applied to the atoms in a channel protein and its pore.

Ionic solutions, semiconductors, and presumably ions in channels fall within the general scope of electrodiffusion (see Rubinstein, 1990, for a survey). Semiconductor device theory also has its analog of the PNP model, termed the self-consistent drift-diffusion model in that subject (see Roosbroeck, 1950). Models allowing energy transfer, and thus temperature changes, are routinely used in semiconductor physics, as they must be if the hot electron effect is to be understood and managed, as it needs to be in small (i.e., micrometer and submicrometer) devices. Bløtekjaer (1970) introduced the moment method to the microelectronics community, based on macroscopic relaxation times, and, in a widely quoted paper, Shur (1976) showed that, by simultaneously solving momentum and energy balance equations with appropriate relaxation terms, one could describe significant hot electron effects.

The hydrodynamic model began to be utilized in the mid-1980s (Rudan and Odeh, 1986). Computations with this model are considerably more involved than those of simpler models such as the PNP equations because the model allows a wide range of behavior. The hydrodynamic model includes possible shock waves and propagating disturbances, indeed much of the behavior of fluids that we observe everyday as weather, fluid flow in our bathrooms, or even waves at the beach. Simple discretization does not necessarily work well for such systems; examples are known in which simple discretization produces bizarre results (Leveque, 1992). Many of these difficulties disappear when transport is slow—negligible over times on the scale of relaxations—when shock formation is prohibited. Even then, however, the underlying shock-producing ability of the system forces the use of the shock-capturing algorithms first used for this purpose by Fatemi et al. (1991b; see also Fatemi et al., 1991a). For this reason we employ a previously developed, essentially nonoscillatory shock-capturing scheme (Shu and Osher, 1989) to permit reliable estimates of the solutions of these equations, and we use that scheme, appropriately modified, here.

System

We present here the equations of the hydrodynamic model:

Conservation of particles: $$n_t + (nv)_x = 0, \tag{1}$$

Conservation of momentum:

$$p_t + (pv + nk_BT)_x = enE - (p/\tau_p), \tag{2}$$

Conservation of energy:

$$w_t + (vw + nvk_BT)_x = envE - \frac{w - \frac{3}{2}nk_BT_0}{\tau_w} + (\kappa nT_x)_x, \tag{3}$$

and the electric field $E = -\Phi_x$ is determined by the

Poisson equation: $$-\epsilon\Phi_{xx} = e(n + n_D), \tag{4}$$

where we use the subscript x for derivatives with respect to x and the above symbols are as follows:

- ϵ dielectric constant of the channel's pore,
- $n_{D_{n_0}}$ distribution of permanent charge on the channel protein,
- n ion concentration in the channel's pore,
- v ion translational velocity in the channel's pore,
- p ion momentum density in the channel's pore, $p = mnv$,
- k_B Boltzmann constant,
- T ion temperature in the channel's pore,
- e electron charge,
- Φ electric potential as a function of position,
- τ_p momentum relaxation time of the ions in the channel's pore,
- w ion energy density, defined by $w \equiv (3/2)nk_BT + (1/2)nmv^2$,
- m mass of the ion,
- T_0 temperature of the channel protein and lipid membrane (see the Discussion section)
- τ_w energy relaxation time of ions in the channel's pore,
- κ thermoconductivity coefficient of the ions, defined by $\kappa \equiv (3\ \mu_0 k_B^2\ T_0)/2e$,
- μ_0 ion mobility in the aqueous solution.

The first equation ensures the conservation of the number of particles. It says that the concentration of particles changes with time solely as the result of drift (flow). The second equation states the conservation of momentum, and the last equation is the conservation of energy. The colli-

sions in the last two equations are approximated as relaxations to values of the equilibrium state. The second terms on the left-hand sides of Eqs. 2 and 3 are due to drift. The third term in Eq. 2 is equal to the change of momentum that is due to the pressure gradient: the mechanical force, contributed from ion–ion interactions and the thermal motion of ions. On the right-hand sides, the first term is the electrical force and the second term is the frictional force (due to ion–channel and ion–water interaction). The electrical force arises from all the charges in the system, viz., 1) the charge applied to the baths that sustains the (externally applied) transmembrane potential, 2) the permanent charge on the channel protein, 3) the mobile charge (ions) in the channel's pore, and 4) induced (i.e., polarization) charge of the several dielectrics. In the energy conservation equation the third term on the left-hand side equals the (local accumulation of) work done by the mechanical force. On the right-hand side the first term is the input of electrical energy into mobile ions by the electrical force, the second term is energy loss because of the frictional force, and the last term is the heat flux into the system.

The velocity of ions v is defined as just the translational velocity, the average over the (statistical) distribution of the velocity (e.g., a displaced Maxwellian). The random velocity referred to above is the actual ion velocity minus the translational velocity. The temperature is defined locally by the energy of random motion of each species, so it has the conventional statistical meaning, and the equipartition theorem is assumed to hold everywhere. The translational velocity gives rise to translational kinetic energy, and the random velocity to random kinetic energy. The internal energy is the average random kinetic energy, which is derived for an independent degree of freedom as $(1/2)k_BT$. This is confirmed by the equipartition theorem. By temperature, we mean the internal energy of ions. The temperatures of different species can be different in general (see the Discussion section and the Appendix). The temperature that we report here is that of ions. Clearly, our theory needs to be extended to include a more realistic description of the atoms surrounding those ions, namely, those of water and the channel protein. In our analysis, their thermal properties are described by temperature-dependent friction terms, characterized by a single critical parameter. A more realistic analysis is possible with the methods involving detailed scattering mechanisms, as is done in Monte Carlo simulations of the Boltzmann equation (Fischetti and Laux, 1988).

This meaning of temperature is closely related to, but should not be confused with, the statistical meaning of temperature derived and interpreted under equilibrium conditions: the wisdom of the classical analysis of equilibrium—that temperature is proportional to the statistical average of kinetic energy—is still valid in nonequilibrium transport systems but now only after the translational component of velocity is subtracted out. That is, the velocity distribution is not the usual Maxwellian. The identification can be made abstractly only after subtraction of the translational velocity in any system with significant transport (see, for example, Eisenberg et al., 1995). In general, the internal energy can contain other forms of energy, such as the electrical polarization energy that is due to polarization of the electron cloud surrounding the ion. In this situation we cannot assign the entire internal energy as ion temperature, although our equations are still valid because we apply the first law of thermodynamics to all forms of energy (see the Appendix).

Boundary conditions

Boundary conditions specify the potentials and concentrations on either side of the channel in terms of the experimentally controlled potential V_{bias} and the intrinsic concentration of ions in the bath n_i:

$$\Phi\left(-\frac{L}{2}\right) = \frac{k_BT}{e}\ln\left(\frac{n_i}{n(-L/2)}\right) + V_{bias}, \qquad \Phi\left(\frac{L}{2}\right) = \frac{k_BT}{e}\ln\left(\frac{n_i}{n(L/2)}\right), \tag{5}$$

$$n\left(-\frac{L}{2}\right) = n_D\left(-\frac{L}{2}\right), \quad n\left(\frac{L}{2}\right) = n_D\left(\frac{L}{2}\right), \tag{6}$$

$$T\left(-\frac{L}{2}\right) = T_0, \quad T\left(\frac{L}{2}\right) = T_0, \tag{7}$$

where L is the length of the channel.

The potentials $\Phi(-(L/2))$ and $\Phi(L/2)$ at the boundaries of the channel have two components. One component is the potential V_{bias}, maintained in the baths by the experimental apparatus; the other component is the built-in or Donnan potentials, produced by the permanent surface charges on either side of the channel protein that are accessible to the ions in the baths (Chen and Eisenberg, 1993b). The latter have been extensively analyzed in the physiological literature (Green and Andersen, 1991).

Flux formulas

In the PNP theory the steady-state flux is evaluated by

$$J = \frac{1}{\int_{-(L/2)}^{L/2} \frac{e^{\Phi(\zeta)}}{D(\zeta)}\,d\zeta}\left[n\left(-\frac{L}{2}\right)e^{\Phi(-L/2)} - n\left(\frac{L}{2}\right)e^{\Phi(L/2)}\right], \tag{8}$$

where D is the diffusion coefficient. In the hydrodynamic model the flux is, however, calculated according to its fundamental definition:

$$J(x) = n(x)v(x) \qquad \text{for all } x \in \left[-\frac{L}{2}, \frac{L}{2}\right]. \tag{9}$$

Empirical formulas for parameters

Little is known and less understood of the movement of ions in solutions under the conditions of interest here, and almost nothing is known or understood about their movement in the pores of proteins under these conditions. Thus, we are forced to describe those motions by the empirical formulas of other fields, chiefly solid-state physics, for which more is known (Baccarani and Wordeman, 1985).

Numerical simulations and theoretical analysis of ionic movement in solutions, joined by direct measurement of ion motion (in the case of proteins), are needed to remedy this situation. The relaxation times τ_p and τ_w are (chiefly) functions of the temperature T and the mobility μ_0. Note that τ_p and μ_0 cannot be set independently. Similarly, the heat conductivity of ion κ depends on mobility and cannot be varied independently, either:

$$\tau_p = \frac{m\mu_0 T_0}{eT}, \tag{10}$$

$$\tau_w = \frac{3}{2}\frac{\mu_0 k_B T T_0}{e v_s^2 (T + T_0)} + \frac{\tau_p}{2}, \tag{11}$$

$$\kappa = \frac{3}{2}\frac{\mu_0 k_B^2 T_0}{e}. \tag{12}$$

Here the typical values of the Parameters are as follows:

ϵ	80.
n_D	~10 mol/l = 6.02 × 10^9/(μm)^3; permanent charge on the channel protein.
n_i	~0.1 mol/l = 6.02 × 10^7/(μm)^3; concentration of ions in the bath.
v_s	0.1 Å/ps, saturation velocity of ions inside the channel's pore.
V_{bias}	[−0.1, 0.1] V; potential difference maintained (experimentally) between the baths.
m	23 a.m.u.; mass of Na^+.
T_0	300 K; ambient temperature of all constituents of the system in the absence of flux of energy or species, etc.
μ_0	4.0 (Å)^2/ps V; mobility of ions in the channel's pore when electric fields and other driving forces are small.
L	25.0 Å; length of the channel.

RESULTS

We evaluate the change in ion temperature during ion permeation under one set of conditions with the permanent charge distribution on the channel protein shown in Fig. 1. We consider only the transport of one ion species, assuming that the channel excludes all others. In later work this restriction will be relaxed, but at the cost of further assumptions, namely, about the coupling of the energy of one species of ion to another. The dimensions and charge distribution resemble the gramicidin-A channel. The (absolute value) of the charge is shown by the dashed curve measured by the right-hand scale in Fig. 1. The (equivalent one-dimensional) charge distribution in this channel's pore (which contains no formal charges, only carbonyl groups) is some 10–100 M, whereas the typical ionic solution is in the millimolar range. The high density of permanent charge allows the channel to govern ion permeation. The channel is 25 Å long and 2 Å in radius. The diffusion coefficient used is 10^{-5} cm^2/s, the value in a free solution. By Einstein's relation, this is equivalent to a value of mobility (μ_0) of 4.0 × 10^{-8} (μm^2)/(ps V).

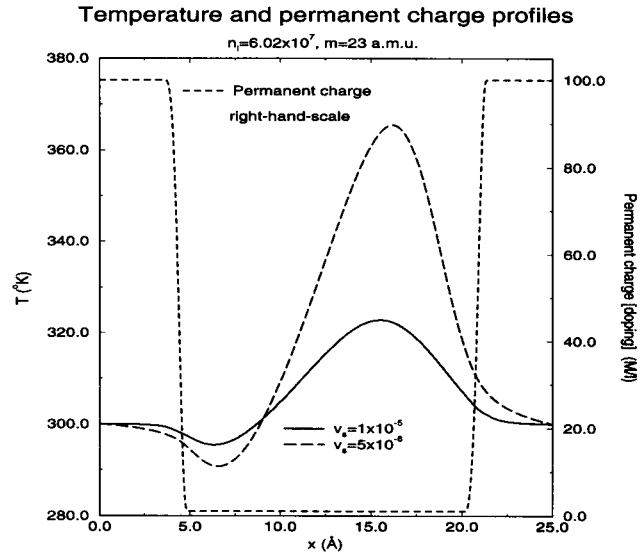

FIGURE 1 Temperature and permanent charge profiles along the ion channel. The solid curve is the temperature profile for $v_s = 1 \times 10^{-5}$, and the long-dashed curve is for $v_s = 5 \times 10^{-6}$. Both temperature profiles are drawn according to the left-hand scale. The short-dashed curve indicates the permanent charge profile drawn according to the scale on the right-hand side. Calculations with different values of the ion diffusion coefficient or different values of the permanent charge at the boundary did not change significantly.

We calculate a channel in a symmetrical ionic solution of 100 mM (i.e., the same on both sides of the cell membrane) and choose a symmetric protein charge profile—purposely not an asymmetric one—only to show that energy exchange and temperature change is not the property of a peculiar channel. Calculations with asymmetric channels and solutions show similar results. Indeed, our conclusions are robust, surprisingly insensitive to all the parameters that we have varied. The conclusions are independent of the details of the doping profile (permanent charge) and of the value of the mobility (the diffusion coefficient): diffusion constants ranging from 10^{-5} to 10^{-7} cm^2/s produce no significant changes in the temperature profile shown in Fig. 1.

The PNP (drift-diffusion) model is the simplest description of the overdamped case, in which collisions are so frequent that their frequency does not matter; i.e., the collision frequency is (effectively) infinite. Less extreme models, such as the hydrodynamic model developed here, need an additional parameter to describe the frequency of collisions, or something equivalent to that frequency. We use the saturation velocity v_s to describe collisions. The saturation velocity is the maximum drift velocity that ions can have; hence, once the saturation velocity is set, so is the relaxation time (as shown in Eq. 11) and also the collision rate. The

saturation velocity is also the ultimate terminal velocity of a particle moving in a viscous medium under an applied force. The more frequent the collisions, the more linear is the dependence of velocity on applied force. That is to say, the more frequent the collisions, the larger is the saturation velocity, because the range of linearity is larger. If the saturation velocity is the independent variable, as it is here, then the larger the saturation velocity, the more frequent collisions are, and the more likely the drift velocity would be proportional to the driving force (for a detailed discussion see Selberherr, 1984, and references therein). Therefore, the larger the saturation velocity, the smaller the temperature rise, because the medium relaxes faster and consequently there is less accumulation of thermal energy. Unfortunately, a molecular analysis of the saturation phenomena or velocity is not available in semiconductors, by simulation or theory, to the best of our knowledge. For that reason, we must rely on phenomenological descriptions (cf. Streetman, 1980; Sze, 1981). Thus, this phenomenon of bulk material—like so many others of experimental importance—is understood qualitatively, but not quantitatively, in molecular or atomic terms. Needless to say, analysis in molecular terms is not available for ions in solutions or channels.

In Fig. 1 we show the temperature profiles of the Na^+ ions computed when the applied transmembrane potential is 100 mV and the saturation velocity has two different values: 10^{-5} μm/ps (10 m/s) and 5×10^{-6} μm/ps. Different values of the saturation velocity describe different types of collision and relaxation processes that consequently yield different temperature profiles. From the reasoning given in the above paragraph, we expect the temperature rise to be lower for $v_s = 10^{-5}$ (the solid curve) than for $v_s = 5 \times 10^{-6}$ (the long-dashed curve), and it is. There is a substantial temperature decrease of the (of course, positive) sodium ions when they decelerate and leave the negatively charged region driven by the externally applied potential difference. On the other hand, sodium ions are accelerated when they enter the negatively charged region approximately three-fifths of the way along the channel. The negatively charged region attracts sodium ions. This acceleration produces a peak in the ion temperature profile. On moving to the right along the x-axis, the temperature tapers off to the ambient temperature set by the applied boundary condition, which reflects the thermal room temperature of the channel protein, the bathing solution, and ultimately the experimental setup. The overall permeation process produces a temperature valley near one-fifth of the way into the channel ($x = 5$ Å) and a peak near three-fifths of the way along the channel ($x = 15$ Å). The temperature valleys and peaks do not coincide in location with the jumps of the permanent charge profiles because electrical interactions (of Coulomb forces) are so long range. The calculation with the permanent charge reduced to 10 M gives almost same feature of the temperature profile, but the temperature rise is reduced because of the reduction in the degree of change of the permanent charge profile.

The parameters τ_p and τ_w determine the relaxation time scale of the system. The typical values are 10^{-14} and 10^{-11} s for τ_p and τ_w, respectively, well in agreement with the time scale of the underlying atomic collisions.

Note that the temperature change computed is ~25°.! This magnitude of temperature change is certainly enough to affect ion permeation, and so we should not ignore or overlook temperature changes or the energy exchanges that produce it.

The magnitude of temperature change is not in hundreds or thousands of degrees, nor is it enough to destroy the membrane when a physiological transmembrane potential is applied. However, if we apply an extreme voltage, say, 500 mV or higher, which are the voltages used to destroy ("zap") a piece of the membrane in whole-cell experiments and in outside-out patches (Hille, 1992), we compute a temperature rise of hundreds or thousands of degrees. Fig. 2 shows such temperature changes when the applied voltage is 500 mV and 1 V (every other parameter remains the same as in Fig. 1). The peak temperature is 650 K for 500-mV membrane potential, and it is 1200 K for 1-V membrane potential. The more the ion temperature deviates from the membrane temperature, the more heat is transferred from ions to the channel protein and the membrane (see the relaxation term in Eq. 3). It would be interesting to see whether this heat transfer (the energy relaxation term) makes T_0 high enough to denature the channel protein. To do this, we need an additional heat equation for T_0 to describe heat diffusion process in the lipid membrane more realistically than in the present analysis, where it is held fixed at T_0.

In Fig. 3, we show the calculated electric potential profiles when the transmembrane potential is 100 mV. The

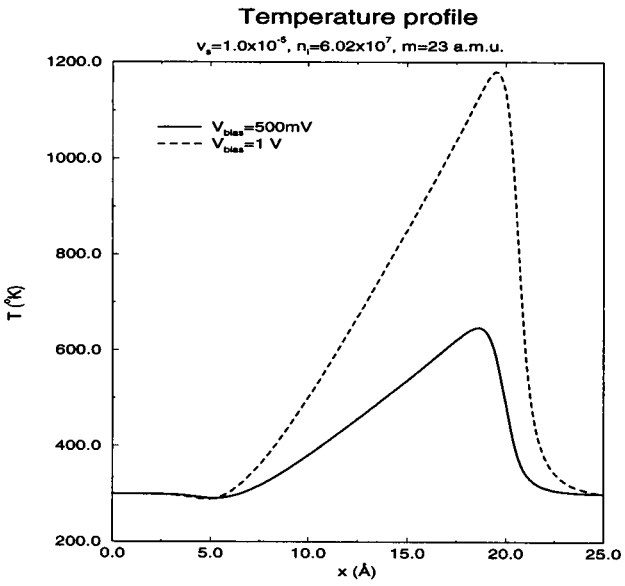

FIGURE 2 Extreme temperature rise when 500 mV and 1 V transmembrane potentials are applied. The solid curve is for the case of 500-mV applied potential, and dashed curve is for that of 1 V. The diffusion coefficients and the ionic concentrations are the same as in Fig. 1.

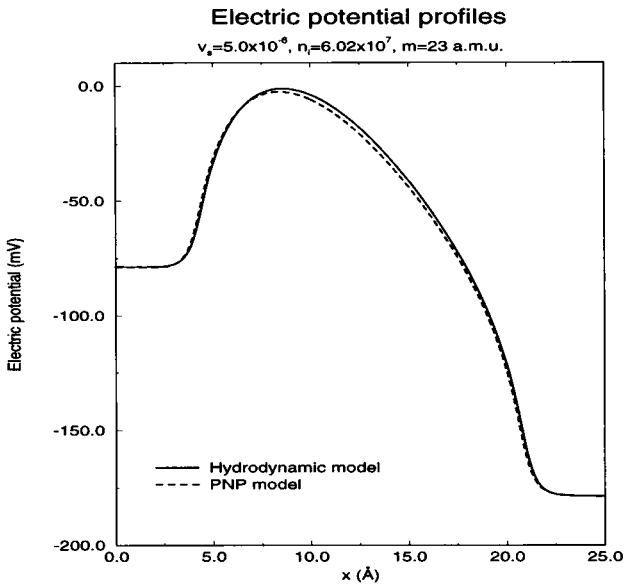

FIGURE 3 Electrical potential profile along the channel when 100-mV transmembrane potential is applied. The solid curve is the result calculated by the hydrodynamic model for $v_s = 5 \times 10^{-6}$, and the dashed curve is calculated by the PNP model. The electric potential profile for $v_s = 1 \times 10^{-5}$ is almost the same as the solid curve when $v_s = 5 \times 10^{-6}$.

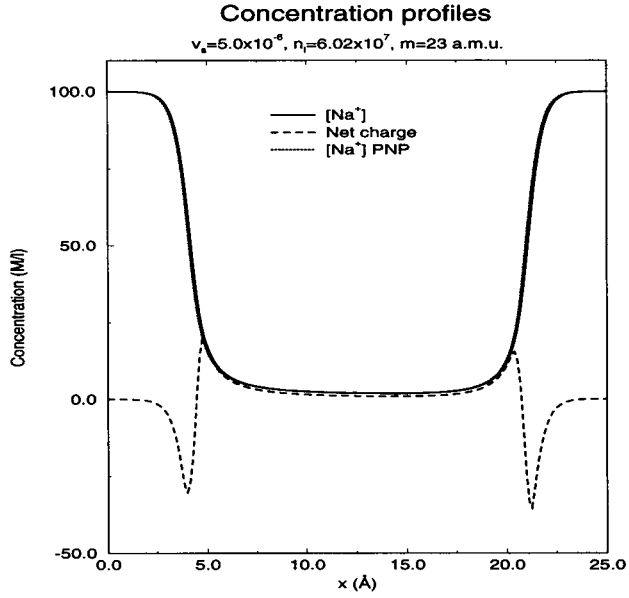

FIGURE 4 Sodium-ion concentration profile and net charge profile along the channel when 100-mV transmembrane potential is applied. The solid curve is the sodium-ion concentration profile calculated by the hydrodynamic model for $v_s = 5 \times 10^{-6}$, the dotted curve is the same sodium-ion concentration profile calculated by the PNP theory, and the dashed curve is the net charge profile. Again, the calculated sodium-ion concentration profile is almost the same for the case when $v_s = 1 \times 10^{-5}$.

solid curve is the output of the hydrodynamic model, and the dashed curve is the result of the PNP equations. These two profiles are quite similar.

The potentials on the right-hand side have not the value of zero (the ground) but a fixed value more negative than the grounded electrode because of the negatively charged channel mouth (which creates a surface potential, namely, the so-called built-in potential, or Donnan potential). The difference of potentials at the left mouth and the right mouth is then the applied transmembrane potential if and only if the channel protein is symmetric (that is to say, if the permanent charge profile is symmetric).

The potential rises (starting from the left-hand side) because the ion enters a more positively (less negatively) charged region there (see Fig. 1). In other words, the potential barrier associated with this more positive region decelerates the motion of sodium ions and produces a small dip in the temperature profile. When ions move farther into the channel, they interact with the adjacent strongly negatively charged region. The potential profile in this region declines with increasing x, eventually reaching the boundary value imposed on the right-hand side by the surrounding bath solution and lipid membrane.

The decrease in the electric potential accelerates the motion of sodium ions along the channel. Therefore, a peak in the temperature profile is formed as shown in Fig. 1. Inside the channel, sodium ions minimize the electrical energy by neutralizing the permanent charges (on the channel protein) as much as possible. That is why the concentration profile of sodium ions (shown as a solid curve in Fig. 4) follows the shape of the permanent charge profile (the doping profile shown in Fig. 1). The physics is controlled by the net charge profile (shown as a dashed curve in Fig. 4). The channel occupancy determines the net charge; consequently it controls the shape of the electric potential profile and eventually controls ion permeation.

These calculations show what we have seen before in the PNP model and has been known in semiconductors for nearly half a century. Any assumption of local electrical neutrality dramatically oversimplifies the situation and eliminates many of the features of ion channel behavior because it locks the active channel in a specific occupancy state by fixing the potential profile. Therefore, the approximation of local electroneutrality forces the active channel into a specific state—a dead state—not responsive to changes of external conditions and not resembling a real channel, or solution to the field equations, whether PNP or hydrodynamic.

Fig. 4 (dotted curve) also shows the concentration profile calculated by the PNP model. The Poisson equation states that the slope of the electric field is related to the local net charge (by a factor of the dielectric constant). Hence, the rise in the net charge profile (dashed curve in Fig. 4) increases the electric field, whereas a decline in the net charge profile will decrease the electric field. This explains the shape of the electric field profile, shown in Fig. 5, which decreases from the left-hand side because of the negatively charged region. Then the positively charged region, which is particularly extended, increases the electric field until the next valley in the net charge profile.

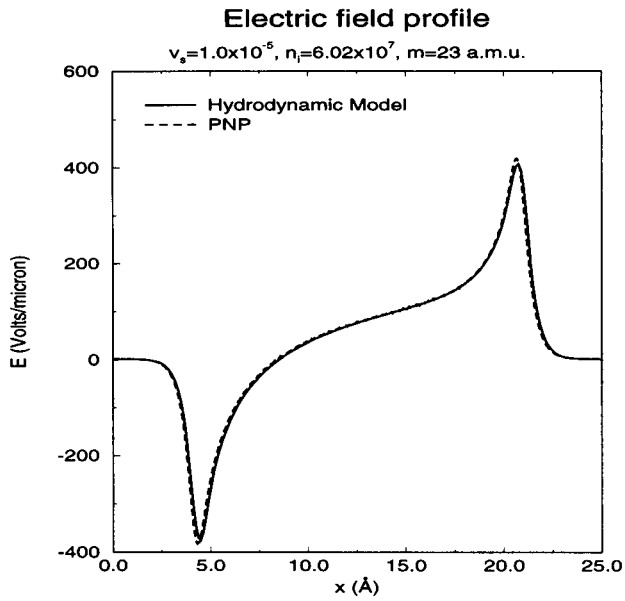

FIGURE 5 Electric field strength profile (solid curve) along the channel when 100-mV transmembrane potential is applied; the dashed curve is the result from PNP. The electric field profiles are not very different for the two models.

In Fig. 6 we show the translational velocity profile of sodium ions across the channel. The solid curve is from PNP, which we calculate by letting $v(x) = J/n(x)$. The long-and-short-dashed curve is for $v_s = 10^{-5}$, the dotted curve is for $v_s = 5 \times 10^{-6}$, and the short-dashed curve is for

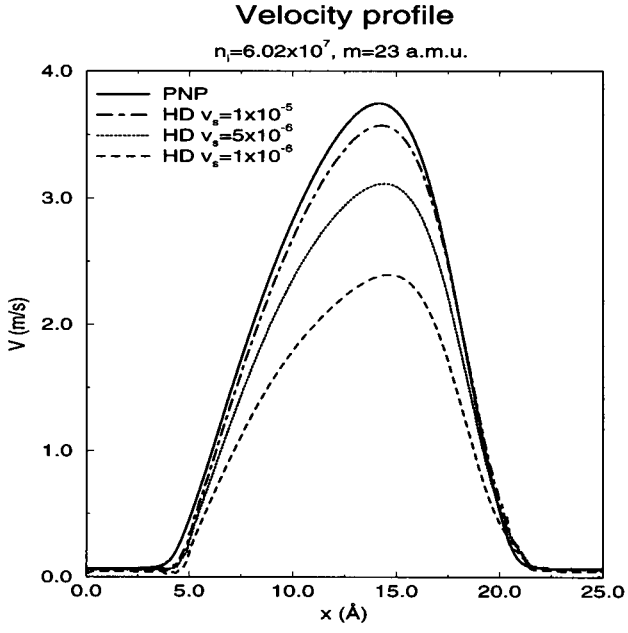

FIGURE 6 Velocity profiles of sodium ions along the channel when 100-mV transmembrane potential is applied. The solid curve is from PNP; the others are the results of the hydrodynamic model with different v_s. The dotted–dashed curve is for $v_s = 10^{-5}$, the dotted curve is for $v_s = 5 \times 10^{-6}$, and the dashed curve is for $v_s = 10^{-6}$.

$v_s = 10^{-6}$. The velocity from PNP has the maximum value among the four velocity profiles, and PNP corresponds to the case of infinite thermal collisions, which enhances the transport process. The smaller the value of v_s, the fewer the thermal collisions and the fewer the ions that are transported (see Fig. 12 below). A pronounced peak coincides with the peak of the temperature profile, which is, of course, nothing but the random component of the ion velocity. The peaks coincide because there is substantial energy exchange between the (mostly deterministic) translational movements of ions through the channel and the random thermal motions in the channel. Fig. 6 demonstrates the existence of substantial energy exchange when ions permeate channels with these characteristics.

We next examine what kinds of energy contribute to the temperature rise of sodium ions. We have already described each term, namely, the mechanical, thermal (heat flux), and electrical energy terms, in the energy equation, Eq. 3. The third term on the left-hand side is the mechanical energy, which is correlated to the ion temperature itself because the pressure of the mechanical energy is proportional to the product of concentration and temperature.

The question then is whether electrical energy or heat flux, or both, contribute to the rise of the temperature reported in Fig. 1. To answer this we have artificially reduced the heat conduction by changing the value of the coefficient κ (of the Wiedemann–Franz law) from 3/2 to 1/2. Fig. 7 shows the results of such a calculation, namely, one with artificially reduced heat flux. The solid curve shows the temperature rise when $\kappa = 3/2$; the short-dashed curve, that for the artificially reduced case of $\kappa = 1/2$; the long-dashed curve, that for doubling the κ to 3. We can see clearly that a 67% reduction in or doubling in heat flux makes only a small difference in temperature profiles. We were surprised by this result because it differs qualitatively from the behavior of semiconductor devices. There, a reduction in κ of some 67% would be sufficient to suppress energy exchange altogether: the spurious velocity overshoot caused by energy exchange would disappear in that case (Jerome and Shu, 1994). This example is quite instructive because it shows the need to analyze a complete set of equations, including a range of energy terms; it is not sufficient to use simply terms that dominate phenomena in other systems, because they may not (and here do not) dominate the phenomena in the system of interest.

Fig. 7 (long-and-short-dashed curve) also shows the temperature profiles for a uniform distribution of permanent charges of 0.1, 1, 10, and 100 M. Interestingly, the temperature profiles are independent of the strength of the uniform permanent charge distribution! This is an immediate consequence of the boundary condition, Eqs. 5, in the one-species model considered here, but it may well not be true in more-general models, including more than one species of ion. In our model, however, the spatial variation of the permanent charge profile plays the key role. If the permanent charge is uniform, the rise in the temperature profiles is only ~3 deg, much less than that found for the nonuni-

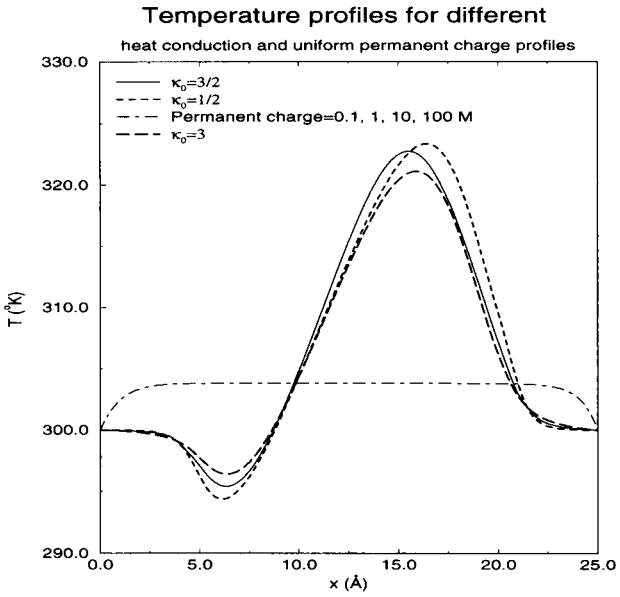

FIGURE 7 Temperature profiles for different heat conduction when 100-mV transmembrane potential is applied. The solid curve is the case when $\kappa = 3/2$ (the ideal value), the short-dashed curve is for $\kappa = 1/2$, and the long-dashed curve is for $\kappa = 3$. The 67% reduction and the doubling of heat conduction make a negligible difference in the temperature profiles, which implies that the ion permeation and heat generation are electrically dominated processes. Results with uniform permanent charges of 0.1, 1, 10, and 100 M are shown by the dotted–dashed curve when $\kappa = 3/2$. The temperature rise is greatly suppressed without the acceleration of ions by the variations of the electric field. This again confirms that heat generation is an electrically dominated process.

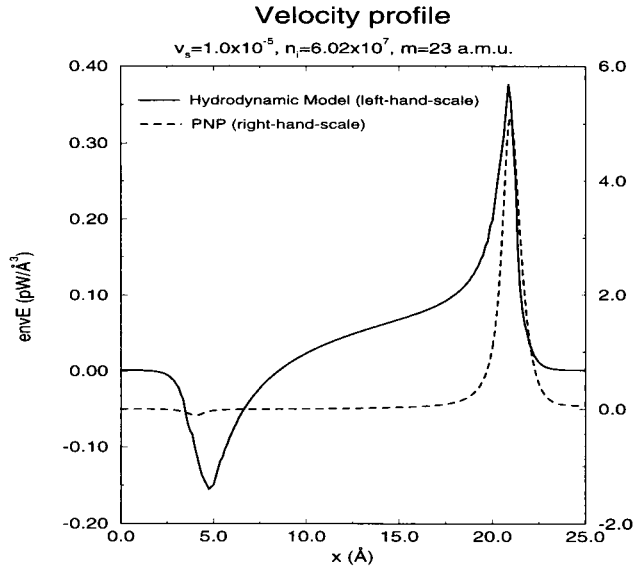

FIGURE 8 Local electrical energy input (solid curve) when 100-mV transmembrane potential is applied. The first term in the energy equation, the local input of electrical energy, is shown to demonstrate that the temperature rise of sodium ions is due to the exchange of the sodium-ion thermal energy and the electrical energy of the applied electric potential. The result from PNP is plotted as a dashed curve according to the scale on the right-hand side.

form distribution of permanent charge (shown in Fig. 1), because the variation of the electric field is much less when the (spatial) variation of the permanent charge is less. When the permanent charge is uniform the variation of the potential profile is much reduced, and so the E term in Eq. 3 is reduced. That is to say, if we reduce the electric energy the first term on the right-hand side, the ion temperature rise, is suppressed. Fig. 7 shows that electrical energy is the source of the temperature rise.

We further confirm our conclusion by plotting the first term on the right-hand side of the energy equation, Eq. 3. The combination *envE* describes the local generation of electric energy, or local input of energy in electrical form (illustrated in Fig. 8). This term is usually called Joule's heating, if all is converted into heat. The small valley, near $x = 5$ Å, coincides with the valley in the temperature profile where the thermal energy (internal energy) of sodium ions is converted into electrical energy because of deceleration of sodium ions. The large peak in Fig. 8 again matches the peak in the temperature profile where the electrical energy is absorbed by the sodium ions and speeds them, raising the sodium-ion temperature as shown in Fig. 6. From Fig. 8 we can see the difference in predicting the usage of the electrical energy by the present model and by the PNP model. The latter is an order of magnitude larger because it is an infinite friction limit. We conclude that ion permeation and temperature rise are both electrically dominated.

For a symmetric channel and uniform diffusion coefficients it is easy to show mathematically that the IV curves are symmetric. Therefore, we restrict the present calculation to $V_{\text{bias}} > 0$.

We now consider a different doping profile (i.e., a profile of permanent charge) and different diffusion coefficients to demonstrate the generality of such energy exchange. A spatially dependent mobility is used in this calculation as suggested by molecular dynamics simulations (Elber et al., 1994) and as shown in semiconductor simulation to be decisive (Jerome and Shu, 1995). In Fig. 9 we show the mobility profile, which starts with a large value in free aqueous solution in the baths and then falls to a smaller value inside the channel, as found experimentally (Dani and Levitt, 1981). Fig. 10 shows a permanent charge profile that varies less than 10 M (in contrast to Fig. 1, where the variation is ~100 M) and the computed temperature profile. The temperature change predicted is more than 40 deg near the channel entrances. Just as in Fig. 1, the temperature changes because of acceleration and deceleration of ions and the concomitant exchange of (mostly deterministic) translational energy and (random) thermal energy.

We conclude that there is substantial energy exchange between the externally applied electrical potential and the internal energy (namely, the temperature) of ions permeating ionic channels, at least in this theory and probably in reality.

In Fig. 11 we show the dependence of the change of temperature on the saturation velocity while the transmembrane potential is held at 100 mV. As stated previously, the

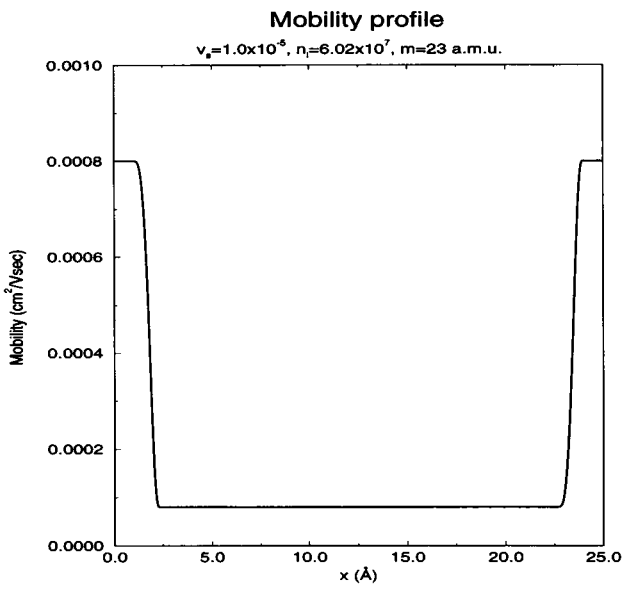

FIGURE 9 Spatially dependent mobility profile used to characterize the difference of bath and channel environments. The values of mobility are equivalent to diffusion coefficients of the order of magnitude of 10^{-5} cm^2/s in the bath and 10^{-6} cm^2/s inside the channel.

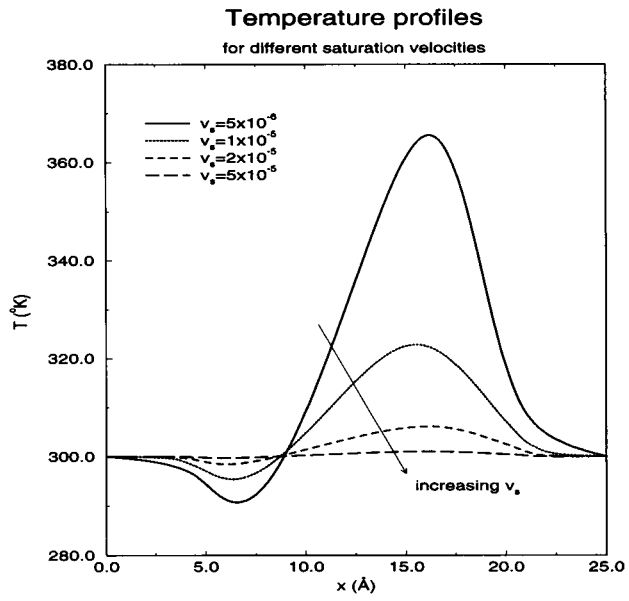

FIGURE 11 Temperature profiles for different values of the saturation velocity. The solid curve is for $v_s = 5 \times 10^{-6}$, the dotted curve is for $v_s = 1 \times 10^{-5}$, the short-dashed curve is for $v_s = 2 \times 10^{-5}$, and the long-dashed curve is for $v_s = 5 \times 10^{-5}$. The rise of temperature is reduced when the value of saturation velocity is increased, corresponding to the case with frequent collisions and an efficient damping of energy exchanges. See the discussion in the Results section.

saturation velocity is a measure of the frequency of collisions: the more frequent the collisions, the less saturation is evident, and so the larger is the saturation velocity. Fig. 11 shows that the significance of the temperature change is gradually reduced when the saturation velocity is increased by an increase in the frequency of collisions. In the figure the solid curve shows the largest change of ion temperature, which occurs when $v_s = 5 \times 10^{-6}$; the dotted curve is an intermediate case with $v_s = 1 \times 10^{-5}$. The shorter-dashed curve shows a smaller change of ion temperature, which occurs if $v_s = 2 \times 10^{-5}$. Finally, the longer-dashed curve shows that almost no change occurs in the ion temperature when $v_s = 5 \times 10^{-5}$. This range of values of v_s, from $v_s = 5 \times 10^{-6}$ to $v_s = 5 \times 10^{-5}$, covers a variety of domains and behaviors. The smallest value, $v_s = 5 \times 10^{-6}$, lies in the domain of the full hydrodynamic model. Under that condition, the full model must be used in computations. The intermediate values, $v_s = 1$–2×10^{-5}, lie within an intermediate domain, often described by a (so-called) adiabatic model in the semiconductor literature. Finally, the largest value, $v_s = 5 \times 10^{-5}$, is in the overdamped domain, where the PNP theory is adequate and temperature changes are insignificant.

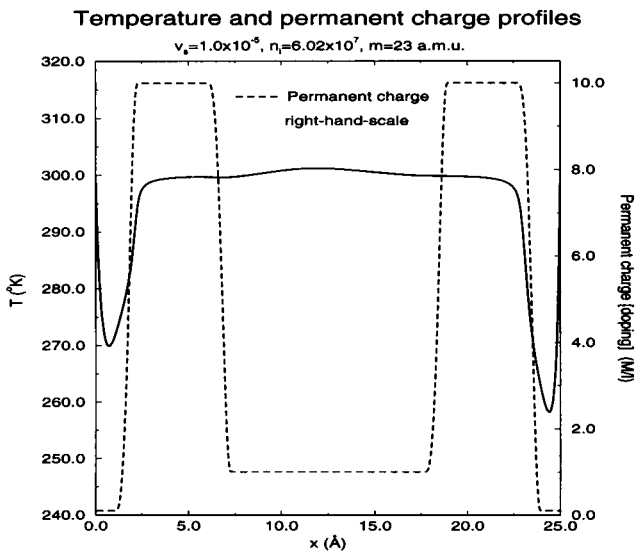

FIGURE 10 Small variation of permanent charge profile and the corresponding ion temperature profile when 100-mV transmembrane potential is applied. The solid curve is for the temperature profile drawn according to the left-hand scale, and the dashed curve is for the permanent charge profile drawn according to the scale of the right-hand side. Other parameters are set to the same values as in Fig. 1.

Fig. 12 shows the IV curve calculated by the PNP theory and the IV curves calculated by the hydrodynamic model for different types of collision (friction). The case with the smaller value of the saturation velocity (namely, the case of less friction) requires the use of the full hydrodynamic equations. A sufficiently large value of the saturation velocity (sufficient friction) reduces the last two equations in the hydrodynamical model to the simple Nernst–Planck equations. When both τ_p and τ_w are sufficiently small the energy equation forces a uniform temperature, and the mo-

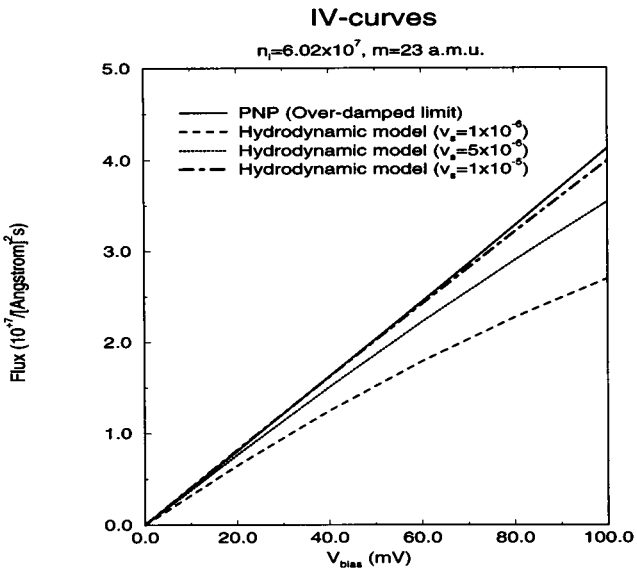

FIGURE 12 Comparison of the hydrodynamic model and the drift-diffusion model (PNP). The IV curves are calculated with the same parameters and geometry but for different choices of the saturation velocity. With the increase of the value of the saturation velocity, the calculated IV curves move from the underdamped limit, passing through the intermediate regime, to the overdamped limit predicted by the PNP model. The solid curve is calculated by the PNP model; other curves are calculated by the full hydrodynamic model. The dashed, dotted, and dotted–dashed curves are for $v_s = 1 \times 10^{-6}$, $v_s = 5 \times 10^{-6}$, and $v_s = 1 \times 10^{-5}$, respectively.

mentum-conservation equation reduces to a Nernst–Planck equation because the term containing the momentum spatial gradient becomes negligible. Physically, this means that collisions are of such short duration that the spatial change of momentum and the relative change of velocity are both negligible, i.e., $|\tau_p v_x| \ll 1$ and $|\tau_p v_t/v| \ll 1$. When there is considerable energy exchange, the deviation between the hydrodynamic and PNP models is quite significant. The PNP model then overestimates the slope by nearly 40%. In Fig. 12 the IV curves are shown only for positive transmembrane potentials because fluxes (currents) are odd functions of the transmembrane potentials (for this particular permanent charge profile). The solid curve in Fig. 12 is calculated with the PNP model; the other curves are calculated from the hydrodynamic model: the dashed, dotted, and dotted–dashed curves for $v_s = 1 \times 10^{-6}$, $v_s = 5 \times 10^{-6}$, and $v_s = 1 \times 10^{-5}$, respectively. The figure clearly shows the transition from general to adiabatic to overdamped domains as the saturation velocity is gradually increased.

The theory just presented has described heat loss to water (and surrounding protein) implicitly by the relaxation term in Eq. 3. Olaf Andersen at Cornell Medical School suggested that we try to include such loss explicitly. That can easily be done by adding a simplified water heat conduction term to the energy equation 3, with the assumptions that 1) the temperature of ions and water molecules equilibrate instantaneously and 2) the heat conduction of water inside the channel obeys the usual Fourier law of heat capacity and conduction. We then have the following:

$$w_t + (vw + nvk_BT)_z = envE - \frac{w - \frac{3}{2}nk_BT_o}{\tau_w} + (\kappa nT_z)_z + \kappa_{H_2O}T_{zz}, \quad (13)$$

where κ_{H_2O} is the thermal conductivity of water, some 0.6 W/K m in bulk (Lide, 1990). Figs. 13 and 14 show the temperature change of the same system described in the previous text but with this water heat conduction term added. Not surprisingly, the instantaneous conduction of heat to water substantially attenuates the temperature change. Fig. 13 shows the case of a transmembrane potential of 100 mV. The water heat conduction attenuates the peak temperature change to ~0.5 deg for bulk thermal conductivity (the dotted-dashed curve) to ~1 deg for κ_{H_2O} = 0.2 W/K m (the dotted–dashed curve) and to ~2.5 deg for κ_{H_2O} = 0.06 (the solid curve), one tenth of the bulk value. Fig. 14 shows a 2-deg peak change for the bulk thermal conductivity (the dotted–dashed curve), an ~4-deg change for κ_{H_2O} = 0.2 (the dashed curve), and a 10-deg change for κ_{H_2O} = 0.06 (the solid curve).

This calculation shows clearly that our results are sensitive to the heat conduction in water and channel protein but that heat conduction is undoubtedly complex and cannot be modeled by an instantaneous loss term independent of time:

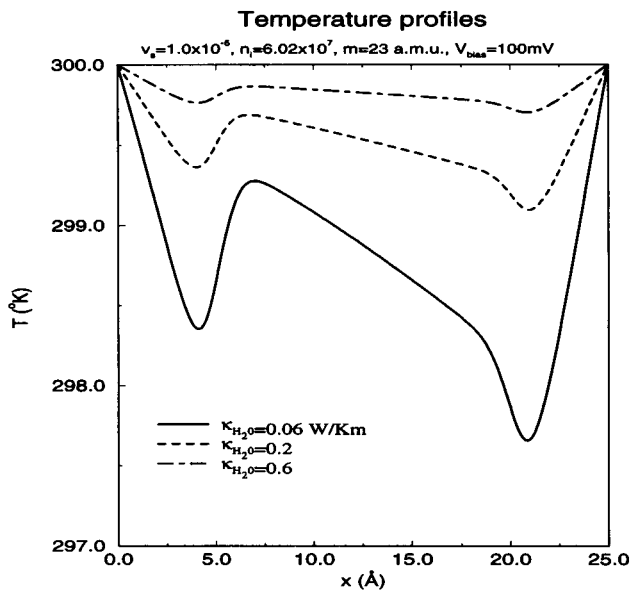

FIGURE 13 Simplified water heat conduction for the transmembrane potential of 100 mV. The calculations are done with the same parameters and geometry but with a water heat conduction term added to the energy equation, assuming 1) the instantaneous temperature equilibrium of water molecules and ions and 2) the usual Fourier law for water heat conduction. The solid, dashed, and the dotted–dashed curves correspond to thermal conductivities of 0.06, 0.2, 0.6 W/K m, respectively. The thermal conductivity in the bulk for water is 0.6.

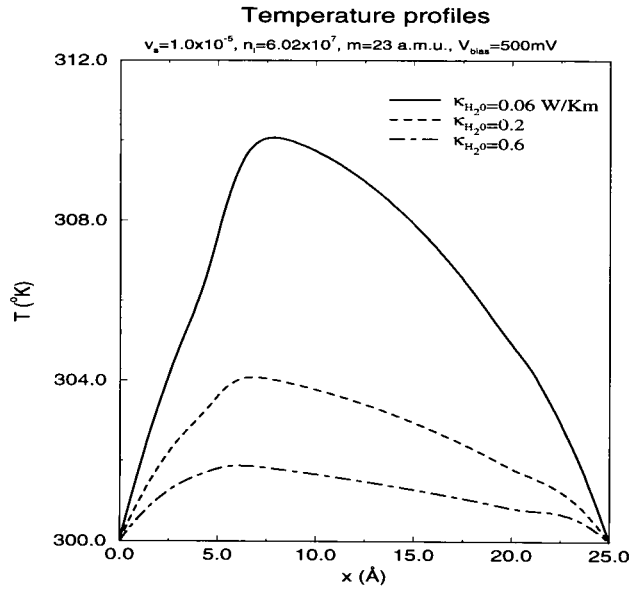

FIGURE 14 Simplified water heat conduction for the transmembrane potential of 500 mV. The same conventions are used as in Fig. 13.

significant, even dominant, motions in solutions occur at 10^{-14} s (Stratt, 1995); large motions occur in proteins from some 10^{-13} s to hundreds of minutes for the slowest conformation changes (Brooks et al., 1988, Table I, p. 19). Indeed, frictional losses in the pore of gramicidin are very different at the maximum and minimum of the potential function and extend over an extremely large time range (Elber et al., 1994). Heat conduction will thus be expected to vary with time, and so will temperature. Again, just as before when we considered the role of the saturation velocity, the lack of experimental information limits the conclusions that we can reach.

DISCUSSION

We show here that a significant temperature change may accompany ion permeation and hope that this theoretical result will motivate further numerical and theoretical analysis and, most importantly, experimental work evaluating the role of temperature change in channel phenomena.

The hydrodynamic theory differs most strikingly from more traditional theories of channels because it allows different species of atoms to have different temperatures (when flux flows, thus away from equilibrium). The existence—indeed, the necessity—of different temperatures (i.e., distribution of velocities) is well known in microscopic theories, including traditional Boltzmann theory (Cercignani et al., 1991) and the more modern (but limited) generalized Langevin theory (Hynes, 1985, 1986; Gardiner, 1985; Hänggi et al., 1990; Fleming and Hänggi, 1993), which (separately or together) are the basis for nearly all theories of condensed matter with atomic resolution, including ionic solutions (Hansen, 1986; Hirschfelder et al., 1954; Rejto et al., 1995; Balian, 1991; Mason and McDaniel, 1988; Horvath, 1985, Chap. 2.15; Adelman et al., 1993). In these theories the distribution of velocities of each species is an output of the theory, a dependent variable that can be spatially uniform and equal (among species) only in the most extraordinary situations. In general, different species flow at different rates, experience different friction, and have different temperatures and thus distributions of velocities. They then have different densities and pressures, so the full set of hydrodynamic and Poisson equations, and conservation laws (Eqs. 1–3), must be used if self-consistency is to be a necessity as well as a virtue.

The existence of multiple temperatures in one condensed phase is an experimental fact in many fields of science. As Mason and McDaniel (1988, p. 224) put it: "... one-temperature basis functions ... failed to produce convergent results at even moderate field strengths, no matter how high the order of approximation. However, the introduction of multitemperature and anisotropic temperature theories has now shown that convergence can be obtained at any field strength. ...

"The idea of multiple temperatures in physical and chemical problems must be quite old. Certainly, it appears repeatedly in diverse connections: electron temperatures in gaseous electronics, plasma physics, semiconductors, and superconductors; rotational and vibrational temperatures in sound absorption, shock-wave phenomena, and chemical kinetics; nuclear spin temperatures in nuclear magnetic resonance; as internal variables in general continuum thermodynamics; and others. Aside from electrons, the concept appears in kinetic theory in connection with the relaxation to equilibrium of a mixture of gases of different masses [six references are cited in the original. To that list, we might add the references to ionic solutions cited previously]. Although collisions soon produce a quasiequilibrium among species of the same mass, the slow interchange of energy between species of different mass on collision gives a much longer time scale for complete equilibrium and justifies the notion of different temperatures for different species."

Here, we strive to add channology to the list of fields that analyze and measure such temperature changes and that do experiments to evaluate their role.

Experimental tests

The idea that temperature change is an essential part of channel function is hardly new: many years ago, heating phenomena in nerves were studied (Howarth, 1975). Unfortunately, this work was severely limited by the available technology. Biological systems (i.e., preparations) with high channel density were not easily available, and the techniques then used had time resolution of seconds and spatial resolution of millimeters (at best); it seems foolhardy now to interpret the early measurements with atomic resolution.

Today, many preparations are known to have very high densities of channels; indeed, many channels can be created at very high density (i.e., overexpressed) by the techniques of molecular genetics. Furthermore, we suspect that tem-

perature measurements can be made today at much higher resolution, in time and distance, and degree(s), than 50 years ago, although we have no personal experience with modern experimental techniques, such as atomic force microscopy (Majumdar et al., 1993), which have the promise of such resolution. Clearly, sensitive measurements of temperature in systems with a high density of channels are needed. A high density of channels occurs at nodes of Ranvier, in electroplaques, and in some neuromuscular junctions and preparations of connexons. Measurements of transporters should be considered as well; transporters occur in high density in many preparations, from the avian salt gland to the sarcoplasmic reticulum of skeletal muscle and, even in the most classical preparation of active transport, in the red blood cell.

Another class of measurements may be possible and indeed has been reported. Measurements of the velocity (distribution) of ions with atomic resolution are made routinely today in physical chemistry. Thus, the report of velocity measurements of the Tl^+ ion in gramicidin channels by laser Doppler velocimetry (Macias and Starzak, 1994) is most welcome. Other physical techniques may also be available. Clearly, experimental measurements are absolutely required to enable us to see whether our predictions occur in real channels. Just as clearly, the help of experimental physical chemists to bring their techniques of temperature (or velocity) measurements into biology, biophysics, and channology is required.

Specific limitations of the analysis

The most serious limitation in this theory is the lack of measurement or simulation of the saturation velocity. Measurements of saturation velocity (in the pores of channel proteins or even in bulk solution) do not exist as far as we are aware. And simulations of nonequilibrium systems are rare: successful ones are nearly nonexistent, to the best of our knowledge, even in simple homogeneous systems over short time spans. Both are needed. Without them, we can only use the parameters of semiconductors, and this is clearly a problem: ions in channels are not electrons or holes in silicon or germanium.

Saturation velocity in semiconductors

The fact that the single parameter of saturation velocity controls the nature of the microscopic collision surprised us because both saturation velocity and momentum relaxation time are important in semiconductor device modeling. Ions are different from the holes and electrons of semiconductors because their momentum relaxation is at least 20 times faster than electrons' (see Eq. 10, where the mass of the electron or hole should be the effective mass when considering semiconductors).

In semiconductor physics the response of drift velocity to increasing field has been observed experimentally in many different semiconductors. In many cases an upper limit is reached in a high field: for most semiconductors, the drift (i.e., deterministic translational) velocity becomes asymptotic to a fixed value close to the mean value of the random thermal velocity. This velocity saturation phenomenon is thought to occur when further energy added by the field is transferred entirely to the lattice and does not stay with the electrons. Unfortunately, we are unaware of any theory that yields this phenomenon as a conclusion in semiconductor physics, electrochemistry, or channology. Nonetheless, theoretical evaluation of the higher moments of the Boltzmann transport equation allowed Hänsch and Miura-Mattausch (1986) to determine the mobility coefficient that produces saturation. At the present time, placing a saturation value in the denominator of the energy relaxation expression is the best way to incorporate the velocity saturation phenomenon in semiconductors.

General limitations of the analysis

Biologists, trained as they are in the chemical tradition, are likely to find the continuum nature of the hydrodynamic theory a problem. After all, matter is made of atoms and not of fluids, and this discrete nature of matter is apparent on the biological length scale.

Continuum analysis is an averaged mean-field representation of atomic reality; where averaged mean-field representations break down, it will too. Continuum analysis has the considerable advantage of depending (mostly) on conservation laws, which are true in any model, atomic or continuum; results that depend on just these are likely to be generally valid. Only experiments can tell what detail of explanation is appropriate. Experimental measurements of temperature in channels are sorely needed.

Implications for previous work

The usual drift-diffusion model is a good approximation only when there is a sufficient water solvation shell to provide many collisions. It clearly is a poor approximation when the translation velocity is high and the full hydrodynamic model is needed to describe fluxes. An intermediate domain also exists where the flux deviates appreciably from the limiting case of drift diffusion, even though the change of temperature of ions is not significant. Within this domain one has to question the validity of the Nernst–Planck flux formula, Eq. 8. Figs. 3 and 4 show that the electrical profile and the ion concentration profile calculated by the PNP theory (in this domain) are not very different from those calculated by the hydrodynamic model when $v_s = 5 \times 10^{-6}$; however, Fig. 12 shows there is still a significant difference between the values of fluxes calculated by Eqs. 8 and 9. The reduction (mapping) of the full hydrodynamic model to the PNP theory is similar to the reduction of the Fokker–Planck equation (a special case of the Boltzmann transport equation) to the Nernst–Planck equation, but it is not at all trivial, requiring, as it does, a realistic description of the saturation velocity.

Biological implications and speculations

The most important result of our calculations is the prediction of possible substantial temperature changes accompanying permeation under a wide range of conditions. The hydrodynamic model combines the electrochemical driving force and thermal temperature driving force and so describes the biological system consistently. More-general combinations of different thermodynamical driving forces and their effects on ion transport are examined by Chen (1994). But theories of the type presented here, which include explicit equations describing energy flow, have other significant advantages. This theory also includes the mechanical pressure tensor as a driving force; hence, our theory may also be used to study the behavior (Sokabe and Sachs, 1992) of stretch-activated channels.

Many biological systems are adequately described experimentally by just their energetics. More-detailed kinetic analysis is not necessary. Indeed, many biochemists have spent their careers showing how chemical energy—nearly always the hydrolysis of ATP—is used to perform essential functions of life in cells. Often, detailed kinetic analysis is superfluous if the goal is to understand qualitative biological function. The work of these metabolic biochemists has shown that a single chemical reaction—the hydrolysis of ATP—is the chemical source of almost all energy used by the cell and its enzymes. The biological use of this energy is remarkably diverse, but its chemical source is unique. Indeed, it is difficult to understand how a single chemical reaction can be coupled to (i.e., "fuel") the diverse reactions that involve so many hundreds (perhaps thousands) of chemical reactions and enzymes. If the fundamental coupling of ATP hydrolysis and metabolism were electrical, the charge and potential on the various substrates would be quite restricted. If the coupling were through heat and temperature, or convection (pressure or volume flow) for that matter, fewer restrictions would apply. Similarly, fewer restrictions would apply if hydrolysis produced a stereotyped conformation change, which is allosterically coupled to remote active sites that themselves have the range of characteristics necessary to accommodate a diversity of substrates and chemical reactions. Of course, the conformation change itself must be fueled by the physical processes of condensed phases—with a concomitant loss in efficiency—namely, by convection, heat flow, diffusion, or migration in an electric field.

One feature of the hydrodynamic model, useful in biological applications, is its explicit treatment of energy: it contains a specific energy equation. Thus, biological sources or sinks of energy can be easily described as just that, namely, an energy source or sink (term) in the appropriate differential equation. The physical basis of that energy gain or loss need not be specified. For example, it is well known that ions experience a drastic change in solvation as they enter channels. How intramolecular forces produce this energy change is not known and will remain difficult to determine on a biological distance and time scale in the presence of flux, even after significant progress in molecular dynamics. The hydrodynamic model requires no such details. It can deal directly with the consequences of the energy change accompanying ion entry into the channel's pore simply by adding an appropriate source term to its energy equation.

In a similar spirit, the energy of ATP hydrolysis can be included directly, as a source of heat just outside (the cytoplasmic end of) a channel (for example), and the consequences for flux can be computed for branched or unbranched channels. Because temperature affects all ions, it is clear that fluxes in such a model will covary and, in that sense, be coupled. What is not clear, until a complete model is studied, is whether such a model can predict the other known properties of ATP-driven active transport.

It is possible that the hydrolysis of ATP fuels all its diverse reactions as we postulate it fuels active transport, namely, by converting chemical energy into a local source of heat, creating a temperature gradient on the atomic distance scale that is then utilized in many different ways. Combustion fuels our civilization in much this way: most of its energy comes from oxidation, from burning carbon to produce heat. How wonderful it would be if the hydrolysis of ATP fueled the specific processes of life by the nonspecific generation of heat, perhaps coupled through conformation changes, just as nonspecific oxidation of carbon fuels the specific tasks of our civilization, sometimes directly, sometimes indirectly, coupled by turbines and generators to current flow in the wires of factories, houses, and computers.

Olaf Andersen made many useful criticisms and suggestions for which we are grateful. DPC would like to thank Prof. Fred Cohen for careful proofreading of this manuscript, to thank Prof. V. Barcilon for useful discussions, and to thank Prof. M. Sokabe for his encouragement of this work. DPC and RSE are supported by National Science Foundation grant BIR-9205688. JWJ, supported by National Science Foundation grant DMS-9123208, is also a visiting professor at the Department of Molecular Biophysics and Physiology of Rush Medical College. CWS is supported by National Science Foundation grant ECS-9214488 and U.S. Army Research Office grant DAAH04–94-G-0205.

APPENDIX

In this appendix we discuss three independent derivations of Eqs. 1–3. These are well known to the community of physical and mathematical scientists but are presented here for completeness, convenience, and perspective as requested by the referees of the paper. These derivations are: 1) by direct application of conservation laws; 2) by the traditional route of (macroscopic) fluid mechanics; and 3) by the more modern (microscopic → macroscopic) moment method.

All the above methods confirm that the system of equations that we use here is correct from the perspectives of fluid mechanics, conservation laws, and microscopic master equations. We proceed directly to the derivations. Some are carried out in an arbitrary number of spatial dimensions (one, two, or three) for completeness.

Conservation equation and Euler's formula

We begin with a general conservation principle, which provides the basis of both derivations 1) and 3). Suppose that a scalar quantity ρ is associated

with a fluid, occupying a spatial domain Ω, where ρ is a volume density, expressed, for illustration, in units of mass or energy per unit volume. Suppose that the flux of the fluid across the boundary of a fixed spatial region $\mathcal{R} \subset \Omega$ is determined as J_ρ. This means that the number of ρ units flowing perpendicularly in a unit time through a unit area of surface of $\partial\mathcal{R}$ is the dot product

$$J_\rho \cdot \nu,$$

where ν denotes the outward unit normal to $\partial\mathcal{R}$. Then the net rate of generation of ρ within $\mathcal{R}$ is equal to the sum of surface integrals and accumulated source/sink term G:

$$-\frac{\partial}{\partial t}\int_{\mathcal{R}} \rho dV = \int_{\partial\mathcal{R}} J_\rho \cdot \nu dA + \int_{\mathcal{R}} G dV. \qquad \text{(A1)}$$

The divergence theorem of vector calculus asserts that the surface integral in (A1) may be written as a divergence volume integral (Friedman, 1971, p. 340):

$$\int_{\partial\mathcal{R}} J_\rho \cdot \nu dA = \int_{\mathcal{R}} \nabla \cdot J_\rho dV. \qquad \text{(A2)}$$

We thus have the volume balance,

$$\int_{\mathcal{R}} -\frac{\partial \rho}{\partial t} dV = \int_{\mathcal{R}} \{\nabla \cdot J_\rho + G\} dV. \qquad \text{(A3)}$$

Because the region $\mathcal{R}$ is arbitrary, the integrands must agree in Eq. A3. We thus have the conservation equation

$$\frac{\partial \rho}{\partial t} + \nabla \cdot J_\rho + G = 0. \qquad \text{(A4)}$$

This equation holds in the entire region Ω of the fluid. Note that G may depend on ρ.

The fundamental starting point, then, is to identify "conserved" quantities, which can be identified with ρ, and to specify their fluxes, J_ρ. If this can be done, then the associated equation is given by Eq. A4.

Next, we state without proof Euler's formula for the total derivative with respective to time:

$$\frac{D}{Dt} = \frac{\partial}{\partial t} + \nu \cdot \nabla. \qquad \text{(A5)}$$

Macroscopic derivation by conservation laws

With Eq. A5, we have that the rate of change of a quantity, say ρ, is

$$\frac{D\rho}{DT} = Flow\_in + External\_input + Output,$$
$$= -\rho v_x + External\_input + Output. \qquad \text{(A6)}$$

One can intuitively identify the first term on the right-hand side of Eq. A6 to be the divergence of the flux and the *External_input* and *Output* to be the source/sink terms. These observations are supported by appeal to the one-dimensional version of Eq. A4.

Conservation of particle number

If there is no generation or recombination, the terms *External input* and *Output* in Eq. A6 are zero. We then have, in one spatial variable,

$$\frac{Dn}{DT} = -nv_x, \quad \text{i.e.,}$$
$$\frac{\partial n}{\partial t} + (nv)_x = 0. \qquad \text{(A7)}$$

Conservation of momentum

Recall that the momentum density is defined as $p = nmv$. If Eq. A6 is applied to momentum, that is, if the substitution $\rho = p$ is made, we get, in one dimension,

$$\frac{Dp}{DT} = -pv_x + External\_input, \quad \text{i.e.,}$$
$$\frac{Dp}{DT} = -pv_x + Total\_force, \qquad \text{(A8)}$$

$$Total\_force = Electric\_force + Mechanical\_force + Frictional\_force, \quad \text{i.e.,}$$
$$= nzeE - P_x - \frac{nv}{\tau_p}, \qquad \text{(A9)}$$

where P is the pressure and the frictional force is approximated by a linear term proportional to, but oppositely directed to, momentum. The symbol z denotes (properly signed) charge number here. By substituting Eq. A9 into Eq. A8 we obtain

$$p_t + (pv)_x = -neE - \frac{p}{\tau_p} - P_x. \qquad \text{(A10)}$$

If we identify the pressure to be

$$P = nk_BT, \qquad \text{(A11)}$$

then Eq. A10 becomes Eq. 2.

Conservation of energy

We now apply Eq. A6 to energy density, that is, we set $\rho = w$ to obtain, in one dimension,

$$\frac{Dw}{DT} = -wv_x + External\_input + Heat\_influx + Work\_done. \qquad \text{(A12)}$$

We know that

$$Heat\_influx = (\kappa nT_x)_x, \qquad \text{(A13)}$$

$$Work\_done = -(Pv)_x, \qquad \text{(A14)}$$

and

$$External\_input = Total force \times velocity, \qquad (A15)$$
$$= \left(nzeE - P_x - \frac{nv}{\tau_p}\right)v.$$

Equation A12 then becomes

$$w_t + (vw)_x = -envE - (Pv)_x - \frac{nv^2}{\tau_p} + (\kappa n T_x)_x. \qquad (A16)$$

Again, if we assume that particles are independent and we use the ideal gas law, Eq. A11 (Huang, 1987), for pressure, Eq. A16 assumes the form of Eq. 3 for the energy relaxation term approximated by a relaxation time.

Macroscopic derivation by fluid mechanics

Conservation of particle number

If we select the ion concentration as the first scalar quantity, *i.e.*, $\rho = n$, the corresponding ion flux is just

$$J_n = nv,$$

where v is the velocity. This gives Eq. 1, via Eq. A4, if we set $G \equiv 0$.

Momentum conservation

We start with Euler's equation (Landau and Lifshitz, 1982):

$$n\left(\frac{\partial v}{\partial t} + v \cdot \nabla v\right) = -\nabla P + nF, \qquad (A17)$$

where F is the sum of all forces except the mechanical force ∇P. Note that specific forces (per unit mass) have been employed. If we add the particle-conservation equation, Eq. 1, dotted by v, to the left-hand side of Eq. A17, we obtain the vector equation

$$\frac{\partial(nv)}{\partial t} + v \cdot \nabla(nv) + (v \cdot \nabla)v = -\nabla P + nF.$$

It remains to identify the force function, F. Here this is represented by an electric force per unit mass:

$$F_{elect} = \frac{e}{m}E,$$

and a frictional force per unit mass:

$$F_{damp} = -\frac{v}{\tau_p},$$

which is a generalization of Stokes's law. Indeed, for a single spherical body of radius a and mass m, moving in a medium with viscosity μ, the classical formula for τ_p is

$$\tau_p = \frac{m}{6\pi\mu a}.$$

Note that $1/\tau_p$ has the dimensions of a frequency, and this is to be interpreted in terms of frequency of collisions, with the resistive force proportional to velocity. Altogether, we obtain Eq. 2 from Eq. A17, with F defined as the sum of F_{elect} and F_{damp}. Goldstein (1957, p. 51) shows how to derive the electrical force from electrical surface tension arguments by means of the Maxwell tensor. In this approach, derived in a so-called laboratory frame, the electrical force does not arise as a source term at all, but as the divergence of the Maxwell tensor.

Energy conservation

The derivation of energy-conservation equation 3 is based on the above momentum-conservation equation and thermodynamic equations. We dot momentum-conservation equation 2 by v, and we get

$$\frac{\partial}{\partial t}\left[\frac{1}{2}mnv^2\right] + \nabla \cdot \left[nv\left(\frac{1}{2}mv^2\right)\right] = -(\nabla P) \cdot v + nmF \cdot v. \qquad (A18)$$

We have also used the conservation-of-particle-number equation in this calculation. The specific force F retains the meaning of the last subsection. To relate the internal energy e_I per unit mass to the thermodynamic quantities, we have to rely on thermodynamic equations, based on the local equilibrium assumption. Let us apply the first law of thermodynamics to a unit volume:

$$nm\, de_I = dQ - PdV, \qquad (A19)$$

where dQ is the heat added to the system and PdV is the mechanical work output of the system. Then the rate of change of the internal energy e_I is

$$nm\frac{De_I}{Dt} = -\nabla \cdot (-\kappa\nabla T) - P\nabla \cdot v. \qquad (A20)$$

On the other hand,

$$nm\frac{De_I}{Dt} = nm\frac{\partial e_I}{\partial t} + mn(v \cdot \nabla)e_I, = \frac{\partial nme_I}{\partial t} + \nabla \cdot (vmne_I), \qquad (A21)$$

where we used the conservation of particle number in the last step. Finally, the rate of change of the internal energy e_I is

$$\frac{\partial nme_I}{\partial t} + \nabla \cdot (vmne_I) = -\nabla \cdot (-\kappa\nabla T) - P\nabla \cdot v. \qquad (A22)$$

By adding Eqs. A22 and A18, we get the energy-conservation equation, Eq. 3.

Moment methods

We have discussed various references for this material in the body of the paper. This is a synopsis of the approach of one of the authors (Jerome, 1995, Chap. 3). We begin with a single-particle master equation for an ion species moving in an electric field:

$$\frac{\partial f}{\partial t} + u \cdot \nabla_x f - \frac{e}{m}E \cdot \nabla_u f = C. \qquad (A23)$$

Here, $f = f(x, u, t)$ is the numerical distribution function of a carrier species' and u is the species' group velocity vector. C is the time rate of change of f that is due to collisions, principally to collisions with the protein. The moment equations, which will be discussed subsequently, are expressed in terms of certain dependent variables, which are now defined.

Fundamental variables as moments

Definition

1) The concentration n is given by the moment integral,

$$n := \int f du.$$

2) The velocity v is given by

$$v := \frac{1}{n}\int uf du.$$

3) The momentum p is given by

$$p := mnv.$$

4) The random velocity c is given by

$$c := u - v.$$

5) The specific pressure tensor P is given by

$$P_{ij} := m\int c_i c_j f du.$$

6) The internal energy density e_I is given by

$$e_I := \frac{1}{2n}\int |c|^2 f du.$$

7) The heat flux q is given by

$$q_i := \frac{m}{2}\int c_i |c|^2 f du.$$

The system

The moment equations, obtained by multiplying the master equation A23 by the functions

$$g_0(u) \equiv 1,$$

$$g_1(u) = mu,$$

$$g_2(u) = \frac{m}{2}|u|^2$$

and integrating, are given by

$$\frac{\partial n}{\partial t} + \nabla \cdot (nv) = C_n, \tag{A24}$$

$$\frac{\partial p}{\partial t} + v(\nabla \cdot p) + (p \cdot \nabla)v = -enE - \nabla \cdot P + C_p, \tag{A25}$$

$$\frac{\partial}{\partial t}\left(\frac{mn}{2}\left|v\right|^2 + mne_I\right) + \nabla \cdot \left(v\left[\frac{mn}{2}\left|v\right|^2 + mne_I\right]\right) + \nabla \cdot (vP) = -env \cdot E - \nabla \cdot q + C_W. \tag{A26}$$

The Poisson equation for the electric potential must be adjoined. Each species contributes a corresponding moment subsystem, with appropriately signed charge. C_n, C_p, and C_w represent moments of C, i.e., integrals with respect to u of the product of C with the functions g_i.

Moment closure and relaxation relations

The system discussed in the preceding subsection has 15 dependent variables in the case of one species in physical space, determined by Φ, n, v, P, e_I, and q. By moment closure is meant the selection of compatible relations among these variables, so that the number of equations is equal in number to variables selected. One way of proceeding is to introduce a new tensor variable T, the effective carrier temperature, defined for independent particles by the ideal gas law relationship

$$P_{ij} = nk_B T_{ij}.$$

and a scalar variable w, the total carrier energy. Reduction to the basic variables n, v, w, and Φ can be implemented by the following assumptions:

Closure assumptions

1) The pressure tensor is isotropic with diagonal entries P_s and off-diagonal entries zero, for a suitable scalar function P_s.

2) It follows from the previous assumption that temperature may be represented by a scalar quantity T and that the internal energy is represented in terms of T by

$$me_I = \frac{3}{2}k_B T.$$

3) The energy w and the heat flux q have the meanings introduced previously in this Appendix, and $q = -\kappa\nabla T$.

Definition

We define the momentum and energy relaxation times, τ_p and τ_w, respectively, in terms of averaged collision moments as follows:

1) The momentum relaxation time τ_p is given through

$$\frac{p}{\tau_p} := -\int muC du := -C_p.$$

2) The energy relaxation time τ_w is given through

$$-\frac{W - W_0}{\tau_w} := \frac{m}{2}\int |u|^2 C du := C_W.$$

Finally, we define $C_n \equiv 0$ if no ions are absorbed or annihilated by the ion channel.

REFERENCES

Adelman, S. A., R. H. Stote, and R. Muralidhar. 1993. Theory of vibrational energy relaxation in liquids: vibrational-translational-rotational energy transfer. *J. Chem. Phys.* 99:1320–1332.

Baccarani, G., and M. Wordeman. 1985. An investigation of steady-state velocity overshoot effects in Si and GaAs devices. *Solid State Electron.* 28:407–416.

Balian, R. 1991. From Microphysics to Macrophysics: Methods and Applications of Statistical Physics. Vol. 1 of Texts and monographs in physics. Springer-Verlag, New York. 465 pp.

Barcilon, V., D. P. Chen, and R. S. Eisenberg. 1992. Ion flow through narrow membrane channels: Part II. *SIAM J. Appl. Math.* 52:1405–1425.

Beris, A. N., and B. J. Edwards. 1994. Thermodynamics of Flowing Systems. Clarendon Press, Oxford. 683 pp.

Bird, G. A. 1994. Molecular Gas Dynamics and the Direct Simulation of Gas Flows. Clarendon Press, Oxford. 458 pp.

Blatt, F. 1968. Physics of Electric Conduction in Solids. McGraw-Hill, New York. 446 pp.

Bløtekjaer, K. 1970. Transport equations for electrons in two-valley semiconductors. *IEEE Trans. Electron Devices.* ED-17:38–47.

Brooks, C. L. III, M. Karplus, and B. M. Pettitt. 1988. Proteins: A Theoretical Perspective of Dynamics, Structure, and Thermodynamics. John Wiley & Sons, New York. 259 pp.

Cercignani, C. 1988. The Boltzmann Equation and Its Application. Applied mathematical sciences. Vol. 67. Springer-Verlag, Wien-New York. 455 pp.

Cercignani, C., R. Illner, and M. Pulvirenti. 1991. The Mathematical Theory of Dilute Gases. Applied mathematical sciences. Vol. 106. Springer-Verlag, Berlin. 347 pp.

Chapman, S., and T. G. Cowling. 1970. The Mathematical Theory of Non-Uniform Gases; an Account of the Kinetic Theory of Viscosity, Thermal Conduction and Diffusion in Gases, 3rd ed. Cambridge University Press, New York. 423 pp.

Chen, D. P. 1994. Nonequilibrium thermodynamics of transports in ion channels. *In* Progress of Cell Research: Towards Molecular Biophysics of Ion Channels. M. Sokabe, editor. Elsevier Science, Amsterdam (in press).

Chen, D. P., and R. S. Eisenberg. 1993a. Charges, currents, and potentials in ionic channels of one conformation. *Biophys. J.* 64:1405–1421.

Chen, D. P., and R. S. Eisenberg. 1993b. Flux, coupling, and selectivity in ionic channels of one conformation. *Biophys. J.* 65:727–746.

Chiu, S.-W., S. Subramaniam, E. Jakobsson, and J. A. McCammon. 1989. Water and polypeptide conformations in the gramicidin channel: a molecular dynamics study. *Biophys. J.* 56:253–261.

Dani, J. A., and D. G. Levitt. 1981. Water transport and ion-water interaction in the gramicidin channel. *Biophys. J.* 35:501–508.

Eisenberg, R. S., M. M. Klosek, and Z. Schuss. 1995. Diffusion between concentration boundary conditions, a stochastic model of an open ionic channel. Part i. *J. Chem. Phys.* 102:1767–1780.

Elber, R., D. P. Chen, D. Rojewska, and R. S. Eisenberg. 1995. Sodium in gramicidin: an example of a permion. *Biophys. J.* 68:906–924.

Fatemi, E., C. Gardner, J. Jerome, S. Osher, and D. Rose. 1991a. Simulation of a steady-state electron shock wave in a submicron semiconductor device using high order upwind methods. *In* Computational Electronics. K. Hess, J. P. Leburton, and U. Ravaioli, editors. Kluwer Academic Publishers, Dordrecht, The Netherlands. 27–32.

Fatemi, E., J. Jerome, and S. Osher. 1991b. Solution of the hydrodynamic device model using high-order nonoscillatory shock capturing algorithms. *IEEE Trans. Computer-Aided Design of Integrated Circuits and Systems* CAD-10:232–244.

Finkelstein, A. 1987. Water Movement through Lipid Bilayers, Pores, and Plasma Membranes: Theory and Reality. Vol. 4 of Distinguished Lecture Series of the Society of General Physiologists. Wiley-Interscience, New York. 228 pp.

Finkelstein, A., and O. S. Andersen. 1981. The gramicidin A channel: a review of its permeability characteristics with special reference to the single-file aspects of transport. *J. Membrane Biol.* 59:155–171.

Fischetti, M. V., and S. E. Laux. 1988. Monte Carlo analysis of electron transport on small semiconductor devices including band-structure and space-charge effects. *Phys. Rev. B* 38:9721–9745.

Fleming, G. R., and P. Hänggi, editors. 1993. Activated Barrier Crossing. Applications in Physics, Chemistry and Biology. World Scientific, Singapore. 327 pp.

Fornili, S. L., D. P. Vercauteren, M. Welti, and E. Clementi. 1984. Water structure in the Gramicidin A transmembrane channel. *Biochim. Biophys. Acta.* 771:151–164.

Friedman, A. 1971. Advanced Calculus. Holt, Rinehart & Winston, New York.

Gardiner, C. W. 1985. Handbook of stochastic methods for physics, chemistry, and the natural sciences, volume 13 of Springer series in synergetics. Springer-Verlag, New York. 442 pp.

Goldstein, S. 1957. Lectures on Fluid Mechanics. Wiley Interscience, New York. 702 pp.

Green, W. N., and O. S. Andersen. 1991. Surface charges and ion channel function. *Ann. Rev. Physiol.* 53:341–359.

Hänggi, P., P. Talkner, and M. Borokovec. 1990. Reaction-rate theory: fifty years after Kramers. *Rev. Mod. Phys.* 62:251–341.

Hänsch, W., and M. Miura-Mattausch. 1986. The hot-electron problem in small semiconductor devices. *J. Appl. Phys.* 60:650–656.

Hansen, J.-P. 1986. Theory of Simple Liquids, 2nd ed. Academic Press, London. 556 pp.

Hille, B. 1992. Ionic Channels of Excitable Membranes, 2nd ed. Sinauer Associates Inc., Sunderland, MA. 607 pp.

Hirschfelder, J. O., C. F. Curtiss, and R. B. Bird. 1954. Molecular Theory of Gases and Liquids. John Wiley & Sons, New York. 1219 pp.

Horvath, A. 1985. Handbook of Aqueous Electrolyte Solutions: Physical Properties, Estimation, and Correlation Methods. Ellis Horwood series in physical chemistry. Halsted Press, New York. 631 pp.

Howarth, J. V. 1975. Heat production in non-myelinated nerves. *Phil. Trans. R. Soc. London Ser. B.* 270:425–432.

Huang, K. 1987. Statistical Mechanics. John Wiley & Sons, New York. 470 pp.

Hynes, J. T. 1985. Chemical reaction dynamics in solution. *Annu. Rev. Phys. Chem.* 36:573–597.

Hynes, J. T. 1986. Theory of chemical reactions. *In* Theory of Chemical Reaction Dynamics. M. Baer, editor. CRC Press, Boca Raton, FL. Chap. 4, 171–234.

Jerome, J. W. 1995. Analysis of Charge Transport: A Mathematical Study of Semiconductors. Springer-Verlag, Berlin.

Jerome, J. W., and C.-W. Shu. 1994. Energy models for one-carrier transport in semiconductor devices. *In* Semiconductors, W. Coughran, J. Cole, P. Lloyd, and J. White, editors. Part II, Vol. 59 of IMA Volumes in Mathematics and its Applications. Springer-Verlag, Berlin, 185–207.

Jerome, J. W., and C.-W. Shu. 1995. The response of the hydrodynamic model to heat conduction, mobility, and relaxation expressions. *VLSI Design.* 3:131–143.

Landau, L. D., and E. M. Lifshitz. 1982. Fluid Mechanics, Vol. 6 of Course of Theoretical Physics. Pergamon Press, New York. 539 pp.

Leveque, R. J. 1992. Numerical Methods for Conservation Laws, 2nd ed. Birkhäuser, Basel. 214 pp.

Levitt, D. G. 1984. Kinetics of movement in narrow channels. *Curr. Top. Membr. Transport.* 21:181–198.

Levitt, D. G., S. R. Elias, and J. M. Hautman. 1978. Kinetics of movement in narrow channels. *Biochim. Biophys. Acta.* 512:436–451.

D. R. Lide, editor, 1990. CRC Handbook of Chemistry and Physics, 71st ed. CRC Press, Boston, MA.

Macias, F., and M. Starzak. 1994. Laser-Doppler scattering for the determination of ionic velocity distributions in channels and membranes. *Adv. Chem. Ser.* 235:401–413.

Mackay, D. H. J., P. H. Berens, and K. R. Wilson. 1984. Structure and dynamics of ion transport through gramicidin A. *Biophys. J.* 46: 229–248.

Majumdar, A., J. P. Carrejo, and J. Lai. 1993. Thermal imaging using the atomic force microscope. *Appl. Phys. Lett.* 62:2501–2503.

Mason, E. A., and E. W. McDaniel. 1988. Transport Properties of Ions in Gases. Wiley-Interscience, New York. 560 pp.

McCourt, F. R. W., J. J. M. Beenakker, W. E. Köhler, and I. Kuščer. 1990. Nonequilibrium Phenomena in Polyatomic Gases, Vol. 2 of International Series of Monographs on Chemistry. Clarendon Press, New York.

Rejto, P. A., E. Bindewald, and D. Chandler. 1995. Visualization of fast energy flow and solvent caging in unimolecular dynamics. Nature (London) 375:129–131.

Resibois, P., and M. Leener. 1977. Classical Kinetic Theory of Fluids. Wiley-Interscience, New York. 412 pp.

Resibois, P., and M. Leener. 1977. Classical Kinetic Theory of Fluids. Wiley-Interscience, New York. 412 pp.

Roosbroeck, W. 1950. Theory of flow of electrons and holes in germanium and other semiconductors. *Bell Syst. Tech. J.* 29:560–607.

Rosenberg, P. A., and A. Finkelstein. 1978. Water permeability of gramicidin A-treated lipid bilayer membranes. *J. Gen. Physiol.* 72:341–350.

Roux, B., and M. Karplus. 1991. Ion transport in a model gramicidin channel: structure and thermodynamics. *Biophys. J.* 59:961–981.

Rubinstein, I. 1990. Electro-Diffusion of Ions, Vol. 11 of SIAM Studies in Applied Mathematics. Society for Industrial and Applied Mathematics, Philadelphia, PA. 254 pp.

Rudan, M., and F. Odeh. 1986. Multi-dimensional discretization scheme for the hydrodynamic model of semiconductor devices. *COMPEL* 5:149–183.

Selberherr, S. 1984. Analysis and Simulation of Semiconductor Devices. Springer-Verlag, Berlin. 293 pp.

Shu, C.-W., and S. Osher. 1989. Efficient implementation of essentially non-oscillatory shock-capturing scheme, II. *J. Comp. Phys.* 83:32–78.

Shur, M. 1976. Influence of nonuniform field distribution on frequency limits of GaAs field effect transistors. *Electron Lett.* 12:615–616.

Smart, O. S., J. M. Goodfellow, and B. A. Wallace. 1993. The pore dimensions of gramicidin A. *Biophys. J.* 65:2455–2460.

Smith, H., and H. H. Jensen. 1989. Transport Phenomena. Clarendon Press, Oxford. 431 pp.

Sokabe, M., and F. Sachs. 1992. Towards molecular mechanism of activation in mechanosensitive ion channels. *In* Advances in Comparative and Environmental Physiology, Vol. 10. Springer-Verlag, Berlin. Chap. 4, 55–77.

Spohn, H. 1991. Large Scale Dynamics of Interacting Particles. Springer-Verlag, New York. 342 pp.

Stettler, M. A., M. A. Alam, and M. S. Lundstrom. 1993. A critical examination of the assumptions underlying macroscopic transport equations for silicon devices. *IEEE Trans. Electron Devices.* 40:733–740.

Stratt, R. M. 1995. The instantaneous normal modes of liquids. *Acc. Chem. Res.* 28:201–207.

Stratten, R. 1962. Diffusion of hot and cold electrons in semiconductor barriers. *Phys. Rev.* 126:2002–2014.

Streetman, B. G. 1980. Solid State Electronic Devices. Prentice-Hall, Englewood Cliffs, NJ. 461 pp.

Sze, S. M. 1981. Physics of Semiconductor Devices. John Wiley & Sons, New York. 868 pp.

Wallace, B. A. 1990. Gramicidin channels and pores. *Annu. Rev. Biophys. Chem.* 1990:127–157.